ORIGINAL ARTICLE

Absolute Resting ^{13}N-Ammonia PET Myocardial Blood Flow for Predicting Myocardial Viability and Recovery of Ventricular Function after Coronary Artery Bypass Grafting

Jiao Wang,[a] Jian-ming Li,[a] Shuai Li,[a] and Bailing Hsu[b]

[a] Teda International Cardiovascular Hospital Nuclear Medicine Department, Tianjin Medical University Clinical Cardiovascular Institute, Tianjin, China
[b] Nuclear Science and Engineering Institute, University of Missouri-Columbia, Columbia, MO

Objective. We aimed to evaluate the feasibility of resting myocardial blood flow (rMBF), quantified with dynamic 13 N-Ammonia (NH$_3$) PET, for identifying myocardial viability and predicting improvement of left ventricular ejection fraction (LVEF) after coronary artery bypass grafting (CABG).

Methods. Ninety-three patients with coronary artery disease (CAD) and chronic LVEF < 45%, scheduled for CABG, had dynamic ^{13}NH$_3$ PET and ^{18}F-FDG PET imaging. The perfusion/metabolism polar maps were categorized in four patterns: normal (N), mismatch (M1), match (M2) and reverse mismatch (RM). The value of rMBF for identifying viable myocardium (M1, RM) and post CABG improvement of LVEF≥8% was analyzed by receiver operating characteristic (ROC) curves. Correlations of rMBF in segments to ΔLVEF post CABG were verified.

Results. Mean rMBFs were significantly different (*N*=0.60±0.14; M1=0.44±0.07, M2=0.34±0.08, RM=0.53±0.09 ml/min/g, *P*<0.001). The optimal rMBF cutoff to identify viable myocardium was 0.42 ml/min/g (sensitivity=88.3%, specificity=82.0%) and 0.43 ml/min/g for predicting improvement of LVEF ≥8% (74.6%, 80.0%). The extent and rMBF of combined M1/RM demonstrated a moderate to high correlation to improved LVEF (*r*=0.78, 0.71, *P*<0.001).

Conclusion. Resting MBF, derived by dynamic ^{13}NH$_3$ PET, may be positioned as a supplement to ^{18}F-FDG PET imaging for assessing the presence of viable myocardium and predicting potential improvement of LVEF after CABG. (J Nucl Cardiol 2022;29:987–99.)

Key Words: ^{13}N-Ammonia · ^{18}F-FDG · Positron emission computed tomography · Coronary artery disease · Myocardial viability · Myocardial blood flow · Coronary artery bypass grafting

988   J. Wang et al.
       Resting MBF for Predicting Myocardial Viability

Journal of Nuclear Cardiology®
May/June 2022

Abbreviations	
AC	Accuracy
AUC	Area under curve
CABG	Coronary artery bypass grafting
CT	Computed X-ray tomography
^{18}F-FDG	^{18}Fluor-2-fluoro-2-deoxyglucose
LVEF	Left ventricular ejection fraction
MBF	Myocardial blood flow
^{13}NH$_3$	^{13}Nitrogen-Ammonia
NPV	Negative predictive value
PET	Positron emission tomography
PPV	Positive predictive value
ROC	Receiver operating characteristic
RPC	Reproducibility coefficient
SRS	Summed rest score

See related editorial, pp. 1000–1002

INTRODUCTION

Patients with severe ischemic left ventricular dysfunction are often considered candidates for aggressive coronary artery revascularization. ^{18}F-FDG PET imaging is the ''gold standard'' for identifying myocardial viability in patients with ischemic cardiomyopathy[1] and is often used to guide surgical or percutaneous interventional management. Many studies have evaluated its accuracy for predicting recovery of cardiac function after revascularization.[2–4] The risk of coronary revascularization is substantially higher in patients with impaired left ventricular function.[5–7] Assessing the presence and extent of dysfunctional but viable myocardium is important for identifying patients who are likely to benefit most from revascularization procedures. The imaging protocol for ^{18}F-FDG PET imaging may be time consuming as it requires patient preparation with glucose loading and insulin injections to maximize myocardial glucose utilization in ischemic myocardium. Not infrequently ^{18}FDG image quality may be suboptimal in patients with poorly controlled diabetes.[8,9] In recent years, absolute quantification of MBF by dynamic PET imaging is used in many laboratories because of improved detection of multivessel coronary artery disease[10–13] and better risk stratification compared to conventional radiotracer myocardial perfusion imaging.[14,15] Several studies have suggested that absolute quantification of resting MBF with PET imaging may be used for distinguishing hibernating and stunned viable myocardium from infarcted myocardium.[16,17] This would provide an alternative diagnostic imaging method for identifying myocardial viability in patients with

chronic ischemic left ventricular dysfunction. The aim of the present study is to assess the value of absolute quantification of resting MBF by dynamic ^{13}NH$_3$ PET imaging for detecting viable and non-viable myocardium and predicting improvement of left ventricular function after CABG.

MATERIALS AND METHODS

Study Subjects

The database of our laboratory was interrogated from May 2016 to September 2018 for patients with a history of myocardial infarction, chronic left ventricular systolic dysfunction, angiographically confirmed coronary artery disease and who were scheduled for CABG and assessment of myocardial viability. A total of 93 patients were identified, 78 males and 15 females, with an age range from 35-77 years. Assessment of myocardial viability by imaging with^{18}F-FDG PET was requested in 75 patients prior to coronary revascularization and in 18 patients because of severe diffuse triple-vessel coronary artery disease that was not amenable to percutaneous intervention. All patients had echocardiographic assessment of left ventricular function before CABG and confirmed with impaired left ventricular ejection fraction (LVEF). Reassessment of LVEF was performed after CABG for all patients. The patient characteristics are shown in Table 1. The design and ethical standards of this study were reviewed and approved by the Institutional Research Board of Teda International Cardiovascular Hospital.

Echocardiography LVEF Reproducibility

Echocardiography was performed using standard two-dimensional views,[3] and LVEF was calculated employing the modified Simpson's rule.[18] Interobserver variability was assessed in 40 patients who were not participants in the present revascularization study. Ten patients were suspected of having coronary artery disease and had previously assessed normal LVEF (> 45%). Ten other patients with known coronary artery disease had known abnormal LVEF ($\leq$ 45%). Twenty additional patients were randomly selected and had unknown LVEF values. Two experienced echocardiographers assessed LVEF of the same patients twice on the same day. Reproducibility coefficient (RPC) for test-retest repeatability was calculated using the conventional formula: RPC = 1.96 × standard deviation of the difference between the two measurements.

Table 1. Patients characteristics

Male/female	78 (84%) /15 (16%)
Age (years±SD, range)	60±8, 35-77
BMI (kg/m^2 ± SD)	26.49±3.50
LVEF (mean, range)	38%, 27-45%
Hypertension	51 (54.8%)
Hyperlipemia	33 (35.5%)
Diabetes mellitus	41 (44.1%)
Smoking	28 (30.1%)
Family history CAD	26 (27.9%)
History of MI	32 (34.4%)
Index coronary angiography:	
Triple-vessel CAD	74 (79.6%)
Double-vessel CAD	12(12.9%)
Single-vessel CAD	7 (7.5%)
Days to reassess LVEF post CABG (days)	176±59

BMI body mass index; *MI* myocardial infarction; *CAD* coronary artery disease (stenosis >50% in any vessel); *LVEF* left ventricular ejection fraction

^{13}NH$_3$ AND ^{18}F-FDG PET/CT SCANS

Both ^{13}NH$_3$ and ^{18}F-FDG radiotracers were produced using a General Electric (GE) Qilin medical cyclotron for generation of ^{13}N and ^{18}F isotopes and synthesized with TRACELAB positron multifunctional chemical synthesizer in our center with ≥ 95% radiochemical purity. All PET imaging was performed on a dedicated PET/CT scanner (GE Discovery NM690) capable of time-of-flight function and 3D data acquisition in list-mode format. The CT portion of PET/CT scanner was utilized for acquisition of CT images for PET attenuation correction. ^{13}NH$_3$ PET and ^{18}F-FDG PET scans were performed on two consecutive days. During the resting portion of the ^{13}NH$_3$ PET scan, an initial CT scout view was acquired to match the position of the heart with the PET field-of-view (FOV), followed by low-dose CT scanning (120 KVp, 15 mA) for PET attenuation correction. Subsequently, 10-15 mCi (370-555 MBq) of ^{13}NH$_3$ was injected intravenously as a bolus 10 seconds prior to the start of ten minutes of dynamic PET acquisition in 3D list-mode format. After ^{13}NH$_3$ dynamic PET acquisition and a 2 minutes wait, ECG-gated perfusion ^{13}NH$_3$ PET with 8 frames per cardiac cycle was performed for 8 minutes. Before ^{18}F-FDG PET imaging, the patient was fasting for at least 6 hours. Glucose loading was performed according to SNM published guidelines.[19] Once blood glucose level was at 6-7 mmol/L, 3∼5 mCi (111∼185 MBq) of ^{18}F-FDG was injected intravenously. Sixty minutes after ^{18}F-FDG injection, ECG-gated PET imaging was performed with 8 frames per cardiac cycle for 8 minutes using the same CT and PET acquisition parameters as for ^{13}NH$_3$ perfusion PET.

All PET images were reconstructed by 3D iterative reconstruction (2 iterations, 24 subsets), incorporating corrections for tissue attenuation, photon scatter, randoms, geometric efficiency and spatial resolution on the vendor provided workstation (Xeleris workstation).[20] CT and PET registration prior to image reconstruction was verified by an experienced technologist with manual adjustment in translational directions. For ^{13}NH$_3$ dynamic PET, the 3D list-mode data were rebinned and then reconstructed to generate dynamic PET images for MBF quantitation. The acquisition sequences for dynamic PET images were as follows: 12 frames at 10 sec each, 2 frames at 30 sec each, 1 frame at 60 sec, and 1 frame at 360 sec for a total acquisition time of 10 minutes. PET images of ^{13}NH$_3$ perfusion and ^{18}F-FDG were reconstructed with the same methodology.

Quantification of Resting MBF

Resting MBF was quantified using dedicated PET blood flow software (QPET, Cedars Sinai, Los Angeles, USA).[21] The software automatically located the left ventricular myocardial region to define left ventricular outline and was applied to all the time frames to generate a time activity curve (TAC) over the myocardium. A blood pool input sampling region of the left ventricle (cylindrical: radius 1.0 cm, long: 2.0 cm) was placed in the middle of the valve plane along the long axis of the heart. According to the dynamic modeling of ^{13}NH$_3$, a two-tissue three-compartment model was implemented, including a compartment inside and outside the vessel and the ^{13}NH$_3$ compartment captured by metabolism to glutamine. The uptake rate is represented by K. The uptake rate of free diffusion of ^{13}NH$_3$ (K_1), the clearance rate of ^{13}NH$_3$ (k_2), the spillover effect of blood to myocardium and the conversion of NH_3 to metabolism-bound ^{13}N-glutamine (k_3) were calculated from numerical fitting of myocardial and blood TACs with the kinetic modeling. Resting MBF (ml/min/g) was directly converted from K_1. For each patient, resting MBF was displayed in the standard ASNC/AHA 17-segment polar map. Global and segmental resting MBF was automatically calculated with the quantitative program.
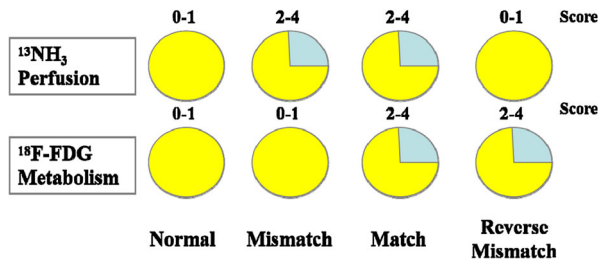
990   J. Wang et al.
       Resting MBF for Predicting Myocardial Viability

Journal of Nuclear Cardiology®
May/June 2022

Figure 1. Schematic Representation of Various Myocardial Perfusion/Glucose Utilization Metabolic Patterns. Top row: ^{13}NH$_3$ myocardial perfusion and semiquantitative score; bottom row: ^{18}F-FDG metabolism and semiquantitative score.

Semi-quantitative Analysis of Myocardial Perfusion and Glucose Utilization (Metabolic) Images

^{13}NH$_3$ perfusion and ^{18}F-FDG images were processed and converted to the ASNC/AHA 17-segment polar maps using a cardiac dedicated software (QPS, Cedars Sinai, Los Angeles, USA). Image analysis was performed using semi-quantitative analysis by polar maps. Relative regional NH$_3$ perfusion was expressed as percent uptake of the maximal uptake in myocardium. For ^{13}NH$_3$ perfusion and ^{18}F-FDG metabolic images, individual segment was scored on a 5-point scale according to the ASNC guidelines[22] as: 0= ≥90% of the maximum uptake; 1 = 75%-89% of the maximum uptake; 2 = 50%-74% of the maximum uptake; 3 = < 50% of the maximum uptake; 4= background. Summed rest scores (SRS) were generated per patient by summing scores in all 17 segments. Each paired segment of ^{13}NH$_3$ perfusion and ^{18}F-FDG images was further categorized into four uptake patterns, according to ASNC guidelines[23] as: (1) normal myocardium: perfusion and metabolism with either 1 or 0 score; (2) mismatch: perfusion score ≥ 2, metabolism score = 0 or 1 (hibernating myocardium); (3) match: both perfusion and metabolism ≥ 2 scores (infarcted myocardium); (4) reverse mismatch: perfusion score = 0 or 1, metabolism score ≥ 2 (stunned myocardium) (Figure 1). Segments that showed a matched pattern (infarcted myocardium) were further subdivided according to radiotracer uptake scores, into ''non-transmural'' infarction (score =2 for perfusion and FDG uptake) and ''transmural'' infarction (score≥3 for perfusion and FDG uptake).[24]

Extent of Areas with Specific Perfusion/ Metabolism Patterns and Mean Resting MBF

In order to reduce a potential error in data analysis, the two basal-septal segments (2 and 3) were excluded from analysis. It is known that using the current version of the quantitative software, MBF may be underestimated due to myocardial sampling error. Thus, a total of 15 segments per patient were included in the data analysis. The extent of an area with a particular perfusion/metabolic pattern was defined as the number of segments involved. Each myocardial segment was expressed as percentage of total myocardium, i.e., 17 segments. Thus, each segment is 100%/17 or about 6% of the total myocardium. Mean resting MBF in a specific myocardial area involving several segments, was calculated as the sum of MBF values within the segments, divided by the number of segments.

Statistical Analysis

The statistical software package SPSS 19.0 (SPSS.inc, IBM, Armonk, NY, USA) was used for data analysis. Non-continuous variables were presented as numbers and percentages. Continuous variables were expressed as mean ± standard deviation with range. Echocardiographic LVEF values were compared by linear regression, and systematic differences were analyzed by the Bland-Altman plot. Difference of resting MBF for each perfusion/metabolism pattern was analyzed with one-way ANOVA statistics. Receiver operating characteristic (ROC) curve analysis was utilized to derive the optimal critical cutoff value (i.e., the point on the curve closest to the upper left corner) of resting MBF that distinguishes best between viable and non-viable myocardium. ROC analysis was also utilized to find the optimal cut-off value of resting MBF that predicts post-CABG improvement of LVEF. Sensitivity, specificity, positive predictive value (PPV), negative predictive value (NPV) and accuracy (AC) were then calculated. A $P<0.05$ was considered statistically significant. The correlation between two variables was analyzed with Pearson correlation. Student T-test was employed to test if existing any difference between two correlation coefficients. $P<0.05$ was considered statistically significant.

RESULTS

Echo LVEF Reproducibility and LVEF Change

The interobserver reproducibility coefficient in patients with LVEF > 45% was 7.7, 7.1 for LVEF ≤ 45% and 7.3 for the randomly selected group, respectively (Figure 2). Consequently, a difference between two LVEF measurements ≥ 8% represents a significant change. Based on this reproducibility assessment, a change of LVEF before and after CABG was analyzed as: LVEF improved (Δ ≥ 8%) and LVEF unchanged (− 8% < Δ < 8%). In 50 patients LVEF improved (Δ ≥ 8%) after CABG, 43 patients had no change of LVEF (−
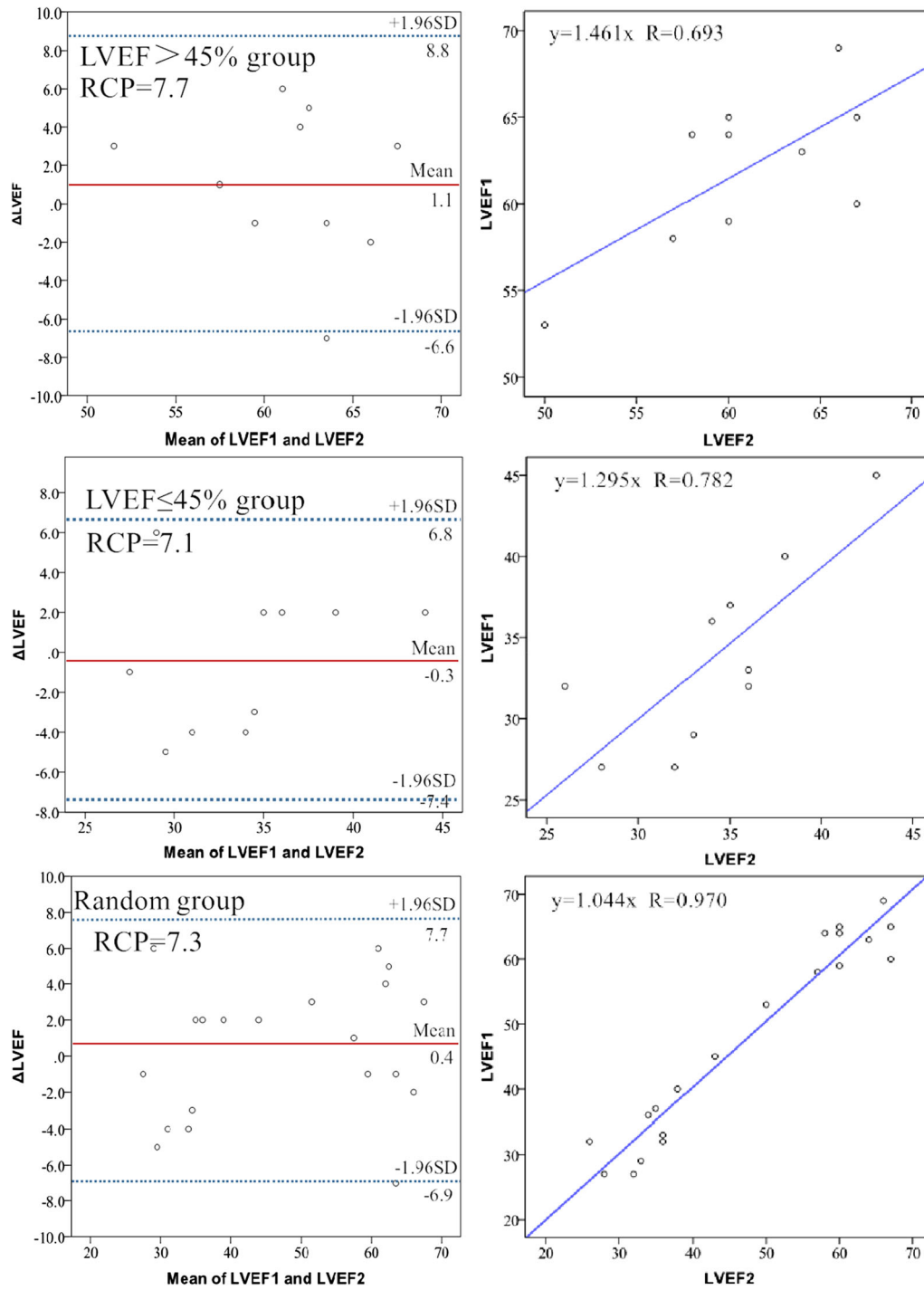
Figure 2. Bland-Altman analysis of interobserver reproducibility of calculation of echocardiographic LVEF. Analysis was performed in three groups of patients with: LVEF $\leq$ 45% (n=10), LVEF >45% (n=10) and 20 random patients with unknown LVEF. The first and second measurements by the two observers were averaged (see text). *RCP* reproducibility coefficient.

992   J. Wang et al.
Resting MBF for Predicting Myocardial Viability

Journal of Nuclear Cardiology®
May/June 2022

Table 2. Change in LVEF after coronary artery bypass grafting in 93 patients with ischemic left ventricular dysfunction

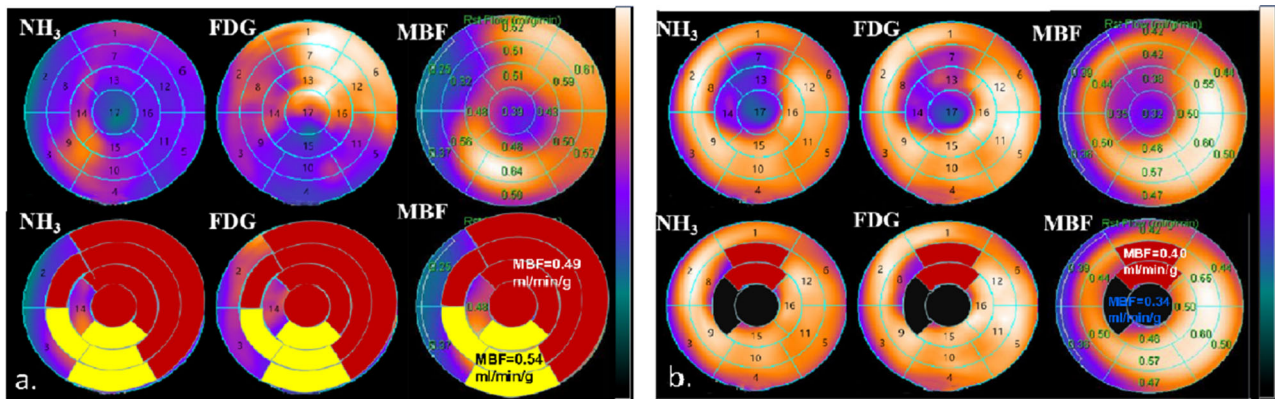| Groups	n (%)	ΔLVEF (%) (mean ± SD, range)
LVEF improved (Δ≥8%)	50 (53.8%)	11±3 (8-22)
LVEF unchanged (-8%<Δ<8%)	43 (46.2%)	3±3 (-4-6)

Figure 3. Polar maps of representative patients. Left: 69-year-old male with coronary angiographic significant stenoses of the left main and all three coronary arteries. Right: 50-year-old male with significant 3-vessel coronary artery disease. The top rows, from left to right shows polar maps of $^{13}NH_3$ myocardial perfusion, ^{18}F-FDG metabolism and Myocardial Blood Flow (ml/min/g). The bottom row shows overlays of colored masks on polar maps in top row: red= mismatch (viable); yellow=reversed mismatch (viable); black=match (non-viable scar).

8% < Δ < 8%) and no patient had deterioration of LV function (Table 2).

Resting MBF in Various Perfusion/ Metabolic Patterns

Of 93 patients with LVEF ≤ 45% (mean: 38±4%, range: 27%-45%), no patients had entirely normal myocardial perfusion images. 15 patients (16.1%) had SRS<4, 33 patients (35.5%) had a SRS=4-9, 30 patients (32.2%) had a SRS=9-14 and 15 patients (16.1%) had a SRS>15. After excluding the two basal segments in each patient, a total of 1395 myocardial segments were available for analysis of segmental myocardial perfusion, glucose metabolism and resting MBF. The correlation between resting perfusion score was − 0.76 (P<0.001). Overall, 785 (56.3%) segments had normal perfusion and glucose utilization, 187 (13.4%) segments showed a mismatch pattern, 245 (17.6%) showed a matched pattern and 178 (12.7%) showed a reverse mismatch pattern. Figure 3 shows two patient examples of $^{13}NH_3$ myocardial perfusion and ^{18}F-FDG metabolic uptake and corresponding absolute resting MBF on 17-segment polar maps. The extents with specific $^{13}NH_3/^{18}FDG$ patterns are identified by colored masks: mismatch=red(viable), match=black (scar) and reverse mismatch=yellow (viable). Figure 4 shows the distribution of resting MBF in 1395 individual segments for each pattern and corresponding mean values and ranges. As shown in Table 3. by one-way ANOVA statistics, resting MBF for each pattern was significantly different from others (P<0.001). As expected, the normal pattern had highest resting MBF (0.60±0.14 ml/min/g) and the match pattern had lowest resting MBF value (0.34±0.08 ml/min/g). Resting MBF values of mismatch and reverse mismatch patterns were between normal and scar values (0.44±0.07 ml/min/g, 0.53±0.09 ml/min/g). In the subgroups with matched uptake patterns, resting MBF of ''transmural'' infarction (0.27±0.06 ml/min/g) was significantly lower than that of ''non-transmural'' infarction (0.39±0.06 ml/min/g) (P<0.001) (Table 4). Interestingly, two subjective and semiquantitative visual
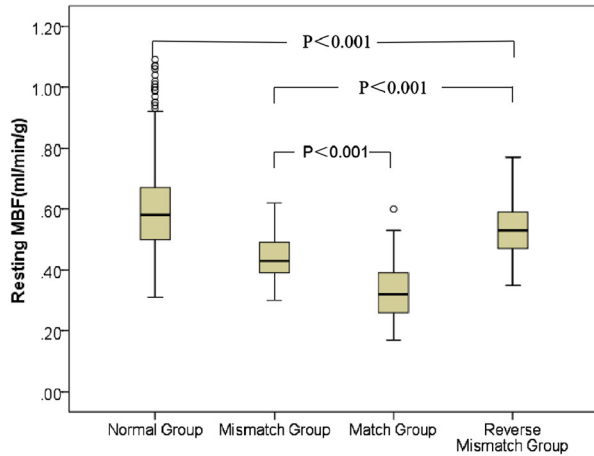
Figure 4. Resting MBF (ml/min/g) in normal segments, mismatched segments, matched segments and reverse mismatched segments. Significances of differences are indicated.

radiotracer uptake scores, i.e., 2 and ≥ 3, quantitatively with significantly different absolute resting MBF. The distribution of resting MBF in match group showed 54.3% overlap with mismatch, 45.0% overlap with reverse mismatch.

Resting MBF and Perfusion Score for Detecting Viable Myocardium

Overall, there were 1150 segments classified as having viable myocardium (i.e., normal, mismatch and reverse mismatch) the remaining 245 segments with matched abnormality were classified as non-viable myocardium. Using the ROC analysis, the optimal cut-off value of resting MBF to distinguish between viable and non-viable myocardium was 0.42 ml/min/g with an area under the curve of 0.94. (Figure 5A). Sensitivity, specificity, PPV, NPV and AC were 88.3%, 82.0%, 89.6%, 83.0%, and 87.5%, respectively. Using a resting MBF value $\geq$ 0.61 ml/min/g, the PPV for detecting viable myocardium was 100%, whereas using a resting MBF value $\leq$ 0.30 ml/min/g the NPV was 100%. For perfusion score, the optimal cut-off value to distinguish between viable and non-viable myocardium was 3 with an area under the curve of 0.96. Sensitivity, specificity, PPV, NPV and AC were 94.7%, 87.0%, 99.2.6%, 63.5%, and 90.3%. (Figure 5B).

Resting MBF for Predicting Improvement of LVEF after CABG

The optimal cut-off value of resting MBF for prediction of improvement of LVEF after CABG was 0.43 ml/min/g with 0.85 area under the curve (Figure 6). Sensitivity, specificity, PPV, NPV and AC were 74.6%, 80.0%, 81.8%, 78.7% and 77.9%, respectively.

Table 3. Resting myocardial blood flow (MBF) in various perfusion/metabolic patterns

Patterns	Myocardial segments n (%)	Resting MBF (ml/min/g)(mean$\pm$SD, range)
Normal	785 (56.3)	0.60±0.14 (0.31-1.24)
Mismatch	187 (13.4)	0.44±0.07 (0.30-0.62)
Match	245 (17.6)	0.34±0.08 (0.17-0.60)
Reverse mismatch	178 (12.7)	0.53±0.09 (0.35-0.77)

Mean resting MBF of each pattern is different from others ($P<0.001$)

Table 4. Mean resting myocardial blood flow (rMBF) in "Non-transmural" and "Transmural" Myocardial Infarction (see text)

Type of infarction	Myocardial segments (n)	rMBF(ml/min/g)(mean$\pm$SD, range)
"Non-transmural"	130	0.39±0.06 (0.25-0.60)
"Transmural"	115	0.27±0.06 (0.17-0.53)

Resting (rMBF): $P<0.001$

994   J. Wang et al.
Resting MBF for Predicting Myocardial Viability
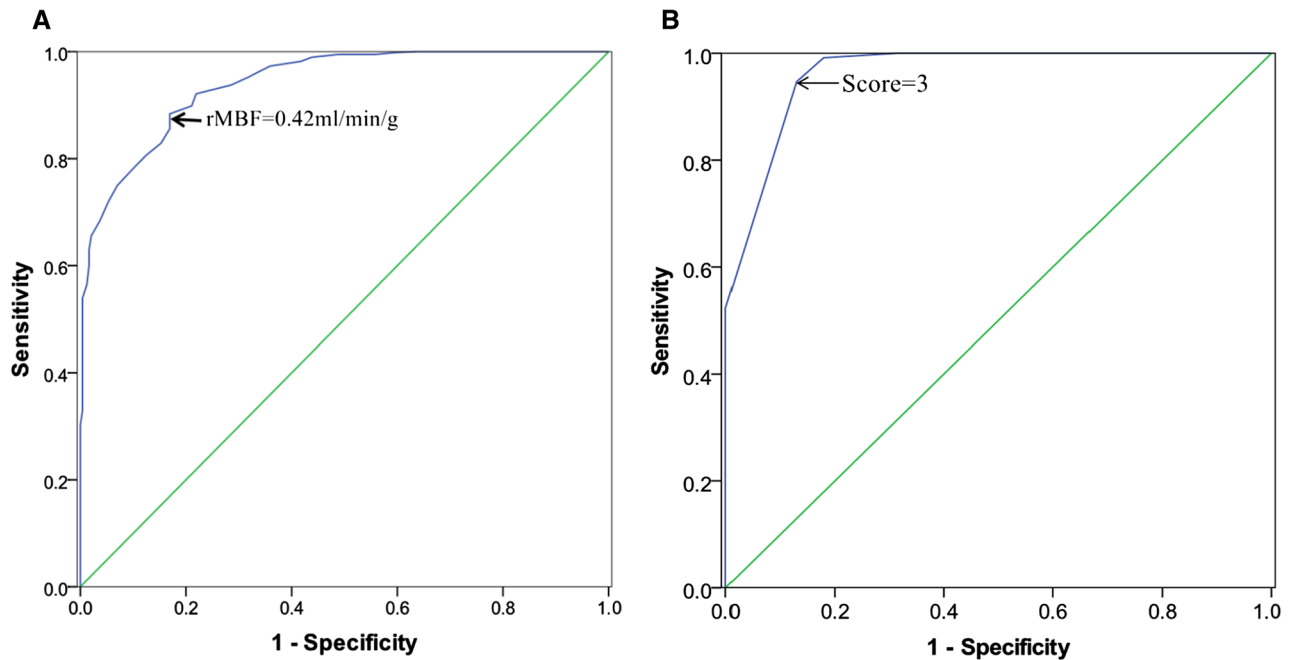
Journal of Nuclear Cardiology®
May/June 2022

Figure 5. AROC curve analysis of resting myocardial blood flow (rMBF) for distinguishing viable myocardium (including normal pattern, mismatch pattern, reverse mismatch pattern) from non-viable myocardium (match pattern). The area under the curve is 0.94. The optimal cut-off value of rMBF is 0.42 ml/min/g. **B** ROC curve analysis of perfusion score for distinguishing viable myocardium from non-viable myocardium. The area under the curve is 0.96. The optimal cut-off value of perfusion score was 3.
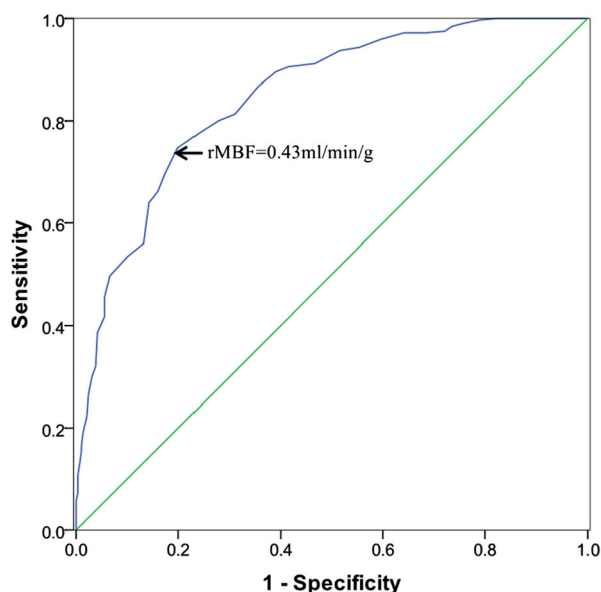
Correlations of LVEF Change Post CABG and Areas in Perfusion/Metabolic Patterns, and Resting MBF

Mean extent and corresponded resting MBF for individual perfusion/metabolic pattern using echocardiography to assess change of LVEF post the revascularization with CABG is shown in Table 5. In the group of 50 patients with improved LVEF ($\Delta \geq 8\%$), extents of mismatch, reverse mismatch and the combine existed moderate to high correlation to LVEF improvement ($r=0.73$, $P<0.001$; $r=0.59$, $P<0.001$; $r=0.78$, $P<0.001$). Resting MBF in the segments overall showed moderate to high correlations with LVEF improvement ($r=0.71$, $P<0.001$; $r=0.65$, $P<0.001$; $r=0.71$, $P<0.001$). Only the extent of match pattern showed negatively moderate correlation to LVEF improvement ($r = -0.59$, $P<0.001$) (Figure 7). In the group of 43 patients with no change in LVEF ($-8\%<\Delta$ and $8\%>\Delta$), both myocardial area and resting MBF for any patterns didn't exist significant correlation to the LVEF change.

Figure 6. ROC curve analysis of resting myocardial blood flow (rMBF) for predicting improvement of global LVEF after coronary artery bypass grafting. The area under curve is 0.85. The optimal cut-off value of rMBF is 0.43 ml/min/g.

Table 5. Mean myocardial area (presented in extent) in perfusion/metabolic patterns and resting MBF correlated with LVEF changes post CABG

	Mismatch		Reverse mismatch		Combined mismatch and reverse mismatch		Match	
	Extent (%)	Resting MBF (ml/min/g)	Extent (%)	Resting MBF (ml/min/g)	Extent (%)	Resting MBF (ml/min/g)	Extent (%)	Resting MBF (ml/min/g)
ΔLVEF≥8%	14.38±7.66 (r=0.73, P<0.001)	0.50±0.05 (r=0.71, P<0.001)	14.76±8.88 (r=0.59, P<0.001)	0.57±0.06 (r=0.65, P<0.001)	29.16±14.19 (r=0.78, P<0.001)	0.54±0.05 (r=0.71, P<0.001)	14.64±10.41 (r=-0.59, P<0.001)	0.35±0.08 (r=0.27, P>0.05)
ΔLVEF<8% and >-8%	8.88±7.14 (r=0.08, P=0.62)	0.44±0.06 (r=-0.14, P=0.42)	9.44±10.65 (r=0.04, P=0.82)	0.52±0.07 (r=0.19, P=0.30)	18.67±11.07 (r=0.12, P=0.43)	0.48±0.06 (r=0.05, P=0.74)	14.26±11.50 (r=0.28, P=0.07)	0.34±0.08 (r=-0.07, P=0.70)

996   J. Wang et al.
Resting MBF for Predicting Myocardial Viability

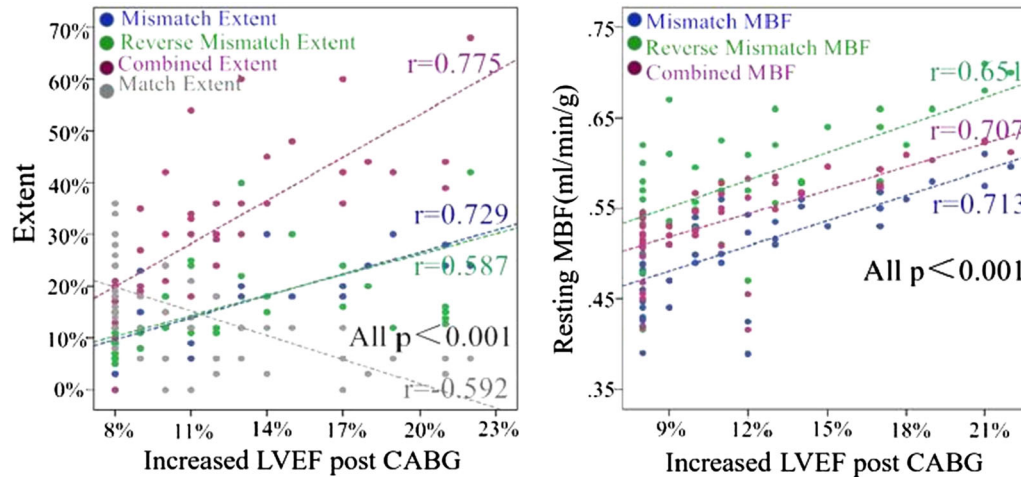Journal of Nuclear Cardiology®
May/June 2022

Figure 7. Scatter plots of mean myocardial area (extent) in perfusion/metabolic patterns and resting MBF correlated with LVEF changes post CABG. The myocardial area of the combined mismatch and reverse mismatch perfusion/metabolic pattern and resting MBF in that area existed moderate to high correlations (r=0.78, 0.71) to LVEF recovery post CABG while myocardial area (extent) of the match pattern showed moderate negative correlations to the degree of LVEF improvement(r=−0.59).

DISCUSSION

The results of our study indicate that regional absolute resting MBF $\geq$ 0.42 ml/min/g and perfusion scores were predictive of the presence of viable myocardium and post CABG improvement of LVEF. Furthermore, the result demonstrated that myocardial area of the combined mismatch and reverse mismatch perfusion/metabolic pattern and resting MBF in that area existed moderate to high correlations (0.78, 0.71) to LVEF recovery post CABG while myocardial area (extent) of the match pattern showed moderately negative correlations to the degree of LVEF improvement (r=− 59, P<0.001). Consequently, this study verified the feasibility of using resting MBF to determine viable myocardium and non-viable myocardium, and to forecast LVEF change by analyzing extent of perfusion/metabolic pattern and resting MBF. Although ^{18}F-FDG without a doubt will remain the standard for assessing viable myocardium, our findings about resting MBF are of clinical relevance. There may exist merits by utilizing dynamic [13]NH$_3$ PET imaging as the supplement to ^{18}F-FDG PET imaging for assessment of viable myocardium as the protocol of measuring absolute MBF by dynamic PET imaging is simpler than the more complex ^{18}F-FDG PET imaging protocol with glucose loading and measuring blood glucose levels. Moreover, in patients with poorly controlled diabetes and insulin resistance, the diagnostic quality of ^{18}F-FDG images is not seldom suboptimal.

Our findings extend and confirm earlier observations about the potential value of resting MBF for predicting myocardial viability.[25–28] Gewirtz et al., in 1994, concluded that using [13]NH$_3$ PET quantification, below a threshold of resting absolute MBF (<0.25 ml/min/g) which myocardial viability was very unlikely preserved. However, Aramayo Gerónimo et al in a small number of patients did not find any correlation between myocardial viability and resting MBF. The study found a comparable range of resting MBF for each pattern, but relatively smaller mean value as compared to the result from our study (normal: 0.69 vs 0.60 ml/min/g; mismatch: 0.50 vs 0.44; match: 0.39 vs 0.33; reverse mismatch pattern: 0.61 vs 0.53). In contrast, Beanlands et al. using similar PET technology as in our study and observed that resting MBF >0.45 ml/min/g was predictive of viable myocardium, with good sensitivity (100%) and specificity (80%). Their findings were consistent with the result of our study, but with relatively smaller sample size to that of our study (n=1395). On the other hand, in a relatively large later study of 180 patients with ischemic cardiomyopathy, Benz et al performed res/stress NH$_3$ MBF and ^{18}F-FDG scans on 180 patients with ischemic cardiomyopathy and divided the myocardium into four types: normal, ischemic, hibernating and scarring. The study concluded that if resting MBF fell below 0.45 ml/min/g, viability testing by ^{18}F-FDG PET may be safely deferred. The study having higher sensitivity (96%) with the literature reported threshold might be attributed to stress MBF and other parameters (e.g., k2 and distribution volume by K1/k2) were

available for data analysis). However, the specificity was negatively impacted (12%). Part of the reasons may be the study select to use a kinetic model only with (K1, k2) and without k3, which could possibly result in a higher K1 value than a standard two-tissue three-compartment model for NH_3. In view of these earlier studies compared with our study, the threshold value of absolute resting MBF > 0.42 ml/min/g to determine viable myocardium as we observed in our study appeared credible

A previous study from Zhang et al.[29] observed a wide range of overlapped resting MBF in viable and non-viable myocardium (0.15-0.81 ml/min/g vs 0.13-0.56 ml/min/g) as viable myocardium can frequently have very low resting MBF. In our study, we observed similar findings (viable: 0.30-0.77 ml/min/g; non-viable: 0.17-0.60 ml/min/g) as the low limit of resting MBF in viable myocardium was slightly higher. In the viable myocardium (defined by mismatch) with low resting MBF, one reasonable explanation may be the myocardial demands only little MBF, particularly, in an akinetic but viable region where the myocardium is in a hibernation state to avoid calcium overload of the mitochondria and thus cell death. In such cases, resting MBF can be quite low due to the metabolic condition and may not be related to the amount of scar tissue. Beanlands et al.[30] used an automated method by dedicated software to determine scar and mismatch scores that considered the score parameters with combination of extent and severity. They found in patients with severe LV dysfunction, the amount of scar was a significant independent predictor of LV function recovery after revascularization. In our study, we found the increased extent of mismatch, reverse mismatch and the combined had moderate to high correlations (0.587-0.775) to LV function improvement while the increased extend of match expressed a negatively moderate correlation (− 0.592). Furthermore, the level of resting MBF in segments of mismatch, reverse mismatch and the combined revealed moderate to high correlations with LV function improvement. These findings may indicate that the extent and the resting MBF in mismatch segments (including the combined) likely can be additional predictors for LV function improvement. However, further studies are needed to confirm this clinical potential.

Absolute quantification of regional MBF may be a practical first step for identifying patients in whom ^{18}F-FDG PET imaging may be useful and in whom it will be not. We found that regional resting MBF ≥0.61 ml/min/g was 100% predictive of viable myocardium, whereas a regional resting MBF <0.30 ml/min/g most likely indicated myocardial scar. The range of resting MBF between these two extreme values may identify

suitable candidates for ^{18}F-FDG viability imaging. In this way quantification of absolute MBF provides complementary practical value in assessing myocardial viability.

LIMITATIONS

Due to a limitation of the quantitative software used in this study, k2 and DV (as K1/k2), kinetic parameters of myocardial washout of $^{13}NH_3$ that are correlated with myocardial viability, were not used in the current analysis. As mentioned above, another limitation is that the extent of a mismatched viable myocardial areas was quantified as a percentage of a polar map, which is confounded by the distorted representation of portions of the left ventricle, e.g., the size of basal segments is overestimated relative to mid-ventricular and apical areas. The semiquantitative method to independently score perfusion and ^{18}F-FDG metabolism for individual segment didn't normalize ^{18}F-FDG uptake with normal perfusion uptake in advance. This missing action likely led to underestimation of the extent of mismatch in an area where mismatch may have mildly reduced perfusion and greatly increased ^{18}F-FDG uptake higher than the normal perfusion area. However, good correlation between the extent of mismatch and improve LVEF post CABG was still observed in our study. Another limitation may be addressed by the binary classification of normal, mismatch, reversed mismatch and match for each individual segment. For those segments with a mixture of mismatch and match, the current approach can't further subcategorize to determine fractions of the two patterns. As addressed by other studies, continuous variables for the analysis of perfusion and ^{18}F-FDG uptake can be utilized as a straightforward solution to this issue giving that a relevant dedicated software is accessible.

CONCLUSION

Resting MBF, derived by dynamic $^{13}NH_3$ PET, may be a suitable supplement to ^{18}FDG PET imaging for assessing the presence of viable myocardium and predicting potential improvement of LVEF after CABG. This alternative imaging methodology may particularly useful in patients with suboptimal ^{18}F-FDG PET image quality.

NEW KNOWLEDGE GAINED

The results of this study suggest that absolute quantification of resting MBF by $^{13}NH_3$ dynamic PET imaging may be a supportive means to distinguish viable myocardium from myocardial scar and predict

998   J. Wang et al.
Resting MBF for Predicting Myocardial Viability

Journal of Nuclear Cardiology®
May/June 2022

improvement of left ventricular function after coronary artery bypass grafting.

Acknowledgements

Conflict of interest

All authors declare that they have no conflict of interest.

References

1. Tillisch J, Brunken R, Marshall R, et al. Reversibility of cardiac wall-motion abnormalities predicted in positron tomography. N Engl J Med. 1986;314:884–8.
2. Nienaber CA, Brunken RC, Sherman CT, et al. Metabolic and functional recovery of ischemic human myocardium after coronary angioplasty. J Am Coll Cardiol. 1991;18:966–78.
3. Marwick TH, Zuchowski C, Lauer MS, et al. Functional status and quality of life in patients with heart failure undergoing coronary bypass surgery after assessment of myocardial viability. J Am Coll Cardiol. 1999;33(3):750–8.
4. Vom-Dahl J, Eitzman DT, Al-Aouar ZR, et al. Relation of regional function, perfusion and metabolism in patients with advanced coronary artery diseased undergoing surgical revascularization. Circulation. 1994;90:2356–66.
5. Christakis GT, Weisel RD, Fremes SE. Coronary artery bypass grafting in patients with poor ventricular function. J Thorac Cardiovasc Surg. 1993;103:1083–92.
6. Elefteriades JA, Tolis G, Levi E. Coronary artery bypass grafting in severe left ventricular dysfunction: excellent survival and improved ejection fraction and functional state. J Am Coll Cardiol. 1993;22:1411–7.
7. Dreyfus GD, Duboc D, Blasco A, et al. Myocardial viability assessment in ischemic cardiomyopathy: benefits of coronary revascularization. Ann Thorac Surg. 1994;57:1402–7.
8. Schinkel AF, Poldermans D, Rizzello V, et al. Impact of diabetes mellitus on prediction of clinical outcome after coronary revascularization by 18F-FDG SPECT in patients with ischemic left ventricular dysfunction. J Nucl Med. 2006;47(1):68–73.
9. Schöder H, Campisi R, Ohtake T, et al. Blood flow-metabolism imaging with positron emission tomography in patients with diabetes mellitus for the assessment of reversible left ventricular contractile dysfunction. J Am Coll Cardiol. 1999;33(5):1328–37.
10. Gerber BL, Vanoverschelde JL, Bol A, et al. Myocardial blood flow, glucose uptake, and recruitment of inotropic reserve in chronic left ventricular ischemic dysfunction. Implications for the pathophysiology of chronic myocardial hibernation. Circulation. 1996;94(4):651–9.
11. Ziadi MC, Dekemp RA, Williams K, et al. Does quantification of myocardial flow reserve using rubidium-82 positron emission tomography facilitate detection of multivessel coronary artery disease? J Nucl Cardiol. 2012;19:670–80.
12. Maddahi J, Packard RRS. PET should replace SPECT in cardiac imaging for diagnosis and risk assessment of patients with known or suspected. CAD: Pro J Nucl Cardiol. 2017;24(6):1955–9.
13. Al-Badarin F, Aljizeeri A, Almasoudi F, et al. Assessment of myocardial blood flow and coronary flow reserve with positron emission tomography in ischemic heart disease: current state and future directions. Heart Fail Rev. 2017;22(4):441–3.
14. Fiechter M, Ghadri JR, Gebhard C, et al. Diagnostic value of 13 N-ammonia myocardial perfusion PET: added value of myocardial flow reserve. J Nucl Med. 2012;53(8):1230–4.
15. Herzog BA, Husmann L, Valenta I, et al. Long-term prognostic value of 13 N-ammonia myocardial perfusion positron emission tomography added value of coronary flow reserve. J Am Coll Cardiol. 2009;54:150–6.
16. Tawakol A, Skopicki HA, Abraham SA, et al. Evidence of reduce resting blood flow in viable myocardial regions with chronic asynergy. J Am Coll Cardiol. 2000;36:2146–53.
17. Prato FS, Butler J, Sykes J, et al. Can the inflammatory response be evaluated using 18F-FDG within zones of microvascular obstruction after myocardial infarction? J Nucl Med. 2015 Feb;56(2):299–304.
18. Schiller NB, Shah PM, Crawford M, et al. Recommendations for quantitation of the left ventricle by two-dimensionalechocardiography. American Society of Echocardiography Committee onStandards, Subcommittee on Quantitation of Two-Dimensional Echocardiograms. J Am Soc Echocardiogr. 1989;2(5):358–67.
19. Dorbala S, DiCarli MF, Delbeke D, et al. SNMMI/ASNC/SCCT Guideline for Cardiac SPECT/CT and PET/CT 1.0. J Nucl Med. 2013;54(8):1485.
20. Vennart NJ, Bird N, Buscombe J, et al. Optimization of PET/CT image quality using the GE 'Sharp IR' point-spread function reconstruction algorithm. Nucl Med Commun. 2017;38(6):471–9.
21. Slomka PJ, Alexanderson E, Jácome R, et al. Comparison of clinical tools for measurements of regional stress and rest myocardial blood flow assessed with 13 N-ammonia PET/CT. J Nucl Med. 2012;53(2):171–81.
22. Dorbala S, Ananthasubramaniam K, Armstrong IS, et al. Single photon emission computed tomography (SPECT) myocardial perfusion imaging guidelines: instrumentation, acquisition, processing, and interpretation. J Nucl Cardiol. 2018;25(5):1784–846.
23. Dilsizian V, Bacharach SL, Beanlands RS. ASNC Imaging Guidelines for Nuclear Cardiology Procedures: Standardized Reporting of Radionuclide Myocardial Perfusion and Function http://www.asnc.org July 2009.
24. Müller-Ehmsen J, Tossios P, Schmidt M, et al. Transmurality of scar influences the effect of a hybrid-intervention with autologous bone marrow cell injection and aortocoronary bypass surgery (MNC/CABG) in patients after myocardial infarction. Int. J. Cardiol. 2012;156(3):303–8.
25. Gewirtz H, Fischman AJ, Abraham S, et al. Positron emission tomographic measurements of absolute regional myocardial blood flow permits identification of nonviable myocardium in patients with chronic myocardial infarction. J. Am. Coll. Cardiol. 1994;23(4):851–9.
26. Aramayo Gerónimo EN, Osorio AR, Geronazzo RJ, et al. Relationship between myocardial viability, myocardial flow and coronary anatomy by positron emission tomography integrated with multislice computed tomography. Rev Argent Cardiol. 2013;81:113–8.

27. Beanlands RS, deKemp R, Scheffel A, et al. Can nitrogen-13 Ammonia kinetic modeling define myocardial viability independent of Fluorine-18 fluorodeoxyglucose? J Am Coll Cardiol. 1997;29(3):537–43.
28. Benz DC, Ferro P, Safa N, et al. Role of quantitative myocardial blood flow and N-ammonia washout for viability assessment in ischemic cardiomyopathy. J Nucl Cardiol. 2019. https://doi.org/10.1007/s12350-019-01684-1.
29. Zhang X, Schindler TH, Prior JO, et al. Blood flow, flow reserve, and glucose utilization in viable and nonviable myocardium in patients with ischemic cardiomyopathy. Eur J Nucl Med Mol Imaging. 2013;40(4):532–41.
30. Beanlands RS, Ruddy TD, deKemp RA, et al. Positron emission tomography and recovery following revascularization (PARR-1): the importance of scar and the development of a prediction rule for the degree of recovery of left ventricular function. J Am Coll Cardiol. 2002;40(10):1735–43.